Superquakes and Supercycles

by Chris Goldfinger, Yasutaka Ikeda, Robert S. Yeats, and Junjie Ren

Online Material: Additional site maps, plots and correlation fits.

INTRODUCTION

The recent 2011 M_w 9.0 Tohoku, Japan, and the 2004 M_w 9.15 Sumatra–Andaman superquakes have humbled many in earthquake research. Neither region was thought capable of earthquakes exceeding $M_w \sim 8.4$. Appealing proposed relationships to predict the size of earthquakes in subduction zones, such as that between earthquake magnitude and parameters such as lower plate age and convergence rate (Ruff and Kanamori, 1980) and plate coupling based on anchored slabs (Scholz and Campos, 1995), at least have many exceptions and may not be valid. Both earthquakes occurred where the subducting plate edge was quite old, ~50–130 Ma. The role of thick sediments smoothing the plate interface and maximizing rupture area has been considered a contributing factor, and it seems to influence many recent great earthquakes (Ruff, 1989). The Tohoku event is also contrary to this hypothesis. Clearly, much remains to be learned about these great events, so much so that most previous estimates of maximum earthquake size in subduction plate boundaries should be considered suspect, and perhaps other fault systems as well (McCaffrey, 2007, 2008).

Our perspective on this issue is clearly hampered by short historical and even shorter instrumental records. The examples noted earlier indicate that basing estimations of maximum earthquake size or models of earthquake recurrence on such short-term records alone clearly cannot encompass the range of fault behavior, even when historical records may be > 1000 years long as in Japan. Here, we present several examples of areas where long geologic and paleoseismic records can illuminate a much wider range of seismic behaviors compared with those deduced from historical and instrumental data, and speculate on models of long-term fault behavior based on very long records.

NORTHEAST JAPAN TRENCH

Since the Pliocene period, the Japan arc has been subjected to east–west compression due principally to the westward convergence of the Pacific plate at the Japan trench at a rate of 82 mm/yr (DeMets *et al.*, 2010). Normal faults, likely resulting from Miocene backarc spreading, have been reactivated in the Plio–Quaternary period as thrust faults due to the change in regional stress fields from tension to east–west compression.

Geologic constraints indicate that this upper-plate compression is only a small fraction of the overall total convergence between Japan and the Pacific plate. Pliocene–Quaternary deformation is concentrated particularly within the Uetsu fold-and-thrust belt and its southern extension, the Northern Fossa Magna, which extend along the Japan Sea coast (Sato, 1989). This fold-and-thrust belt develops within a rifted basin developed during the middle Miocene period in conjunction with the opening of the Japan Sea (Sato, 1994). The rate of horizontal shortening over the Uetsu fold-and-thrust belt during the Pliocene–Quaternary period has been determined to be 3–5 mm/yr (Okada and Ikeda, 2012). Including other active faults and folds, the total rate of horizontal shortening over the northeast Japan arc is estimated to be 5–7 mm/yr, in good agreement with previous estimates (Wesnousky *et al.*, 1982). Deformation to the west in the Japan Sea is thought to be minor based on marine seismic reflection data and seismicity (Okada and Ikeda, 2012) and Global Positioning System (GPS) data that suggest little relative motion between the west coast of northeast Japan and stable Eurasia (Sagiya *et al.*, 2000). Inelastic deformation of the submarine forearc is weakly extensional for the most part (i.e., von Huene and Lallemand, 1990). This indicates that only a fraction (< 10%) of plate convergence is accommodated in the Japan arc as inelastic, permanent deformation. The geologically inferred uplift rate average over the northeast Japan arc during the late Quaternary period is 0.22–0.36 mm/yr (Tajikara, 2004; Tajikara and Ikeda, 2005). If the northeast Japan arc is in isostatic balance, then regional uplift/subsidence occurs due to (1) crustal thickening, which in turn is caused by crustal shortening and magmatic underplating/intrusion; (2) surface unloading by denudation; and (3) surface loading, which resulted from deposition of volcanic and eolian materials. The total rate of crustal shortening was determined from the regional uplift data by eliminating the other disturbing factors and was found to be < 6–8 mm/yr (Tajikara, 2004), in good agreement with the shortening rate deduced from the active fault and fold data.

The geodetically observed, short-term deformation rate within the northeast Japan arc is, however, significantly larger than the long-term deformation rate. Triangulation, trilateration, and GPS observations during the last ~100 years revealed that the Japan arc has contracted in an east–west direction at a rate as high as several tens of millimeters per year (Hashimoto,

 doi: 10.1785/0220110135

1990; Sagiya *et al.*, 2000; Suwa *et al.*, 2006). This rate is nearly one order of magnitude greater than geologically observed shortening rates and is comparable with the ~82 mm/yr rate of plate convergence at the Japan trench (Fig. 1).

Similarly, there is a contrast between recent rapid coastal subsidence and the long-term evidence of terrace uplift along the Pacific coast of northeast Japan. Tide-gauge data indicate abnormally high rates (several to 10 mm/yr) of subsidence during the last ~80 years (Kato, 1983; Fig. 1). This subsidence is likely due to strong coupling dragging down the upper plate by the subducting Pacific plate beneath the Japan arc. However, late Quaternary marine terraces developing along the Pacific coast indicate uplift at 0.1–0.4 mm/yr (Koike and Machida, 2001). The discrepancy between short-term (geodetic) and long-term (geologic) observations indicates that most of the strain accumulating in the last ~100 years has been elastic, to be released by slip in large earthquakes on the subducting plate boundary. Only a fraction of the strain would remain in the arc as inelastic deformation. Although large thrust-type earthquakes with magnitude 7–8.4 have occurred at the Japan

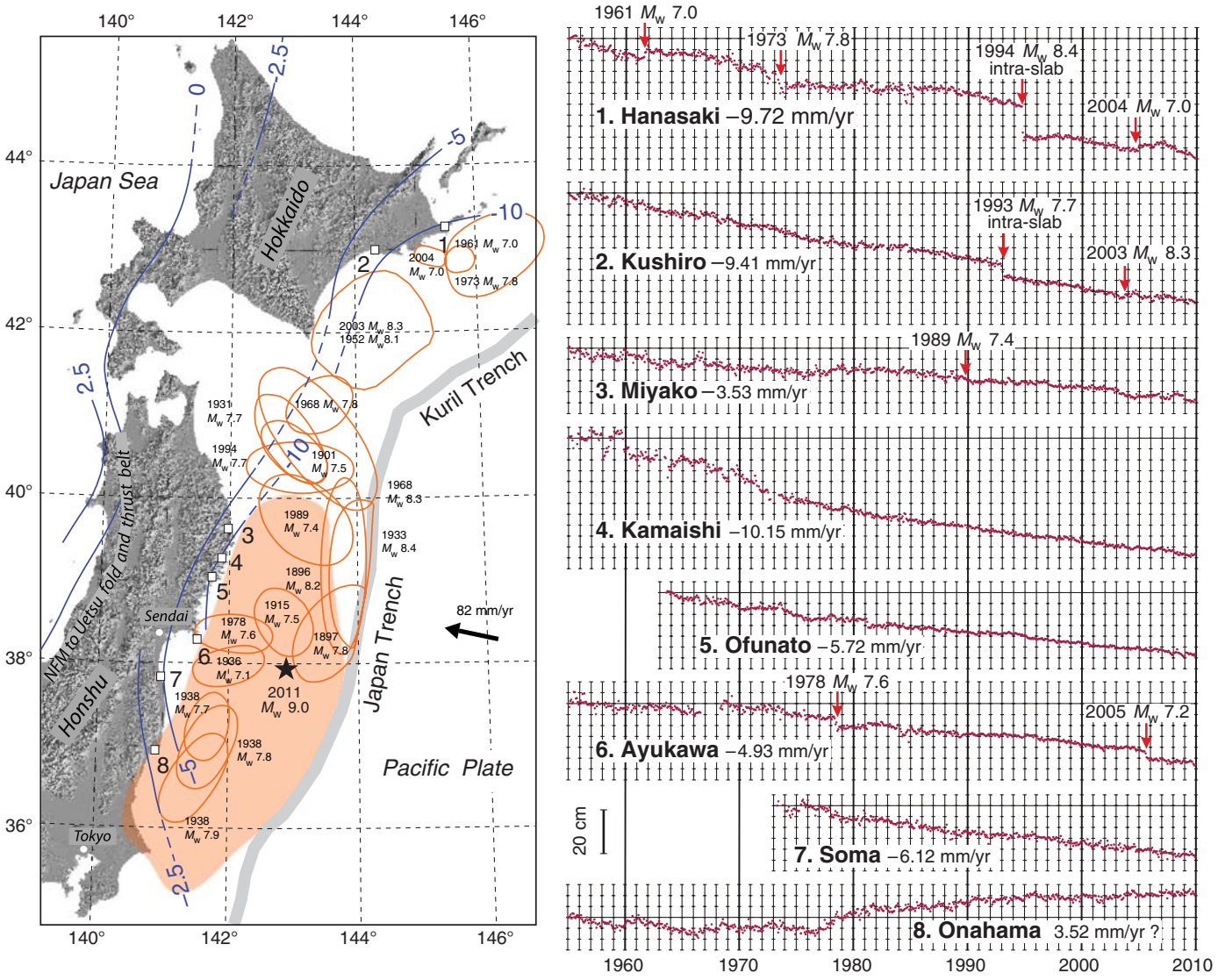

▲ **Figure 1.** (Left) Map showing the recent vertical crustal movements and source areas of large interplate earthquakes. Blue line contours indicate rates of subsidence (in millimeters per year) revealed by tide-gauge observations during the period 1955–1981 (Kato, 1983). Orange lines indicate source areas of interplate earthquakes of M_w >7 since 1896. The epicenter and source area of the 2011 Tohoku earthquake of M_w 9.0 are indicated by a star and orange shade, respectively. NFM, Northern Fossa Magna. Open squares indicate tide-gauge stations; station numbers correspond to those in the right figure. (Right) Selected tide-gauge records along the Pacific coast (Geographical Information Authority of Japan, 2010). See the left figure for location. Red arrows indicate large earthquakes (M_w >7.0) that occurred near each station. Note progressive subsidence of the Pacific coast at rates as high as 5–10 mm/yr, except for the Onahama station, which has likely been affected by coal mining.

trench during the last 100 years, they did not result in significant strain release on land. Thus, larger slip events are required to occur at intervals much longer than the period (~100 years) of instrumental observations (Ikeda, 2003, 2005). The recent Tohoku-oki M_w 9.0 earthquake was such a slip event, with a slip based on submarine GPS of ~24 m (Sato, 2011) and slips greater than 50 m near the toe of the accretionary prism (e.g., Fujiwara *et al.*, 2011); its rupture area encompassed those of numerous previous earthquakes of magnitude 7–8.4 (Fig. 1). A deficit of slip was also inferred in this region from sequences of small repeating earthquakes (Igarashi, 2010). The fact that both the smaller earthquakes and the 2011 earthquake all caused coastal subsidence as well is likely related to deeper coupling that was not released coseismically (Ikeda, 2012).

The most recent earthquakes in the Sendai area, 1933 (M_w 8.1), 1936 (M_w 7.5), and 1978 (M_w 7.6), did not leave a tsunami record in nearby Suijin-numa, a coastal lake (Sawai *et al.*, 2008); neither did they leave extensive sand sheets on the Sendai Plain (Minoura *et al.*, 2001). However, the older historical record in the Tohoku region in Japan includes a number of large earthquakes and associated tsunami, including large events in 869, 1611, and 1896. The largest of these events was likely the 869 Jogan tsunami based on the presence of tsunami deposits in the coastal lake (Sawai *et al.*, 2008), the 3–4 km landward extent of inundation relative to the paleoshoreline (Sawai *et al.*, 2007; Shishikura *et al.*, 2007; Sugawara *et al.*, 2012), and tsunami modeling (Namegaya *et al.*, 2010). The landward inundation of the March 2011 tsunami similarly penetrated 3–4 km inland on the Sendai Plain (http://earthobservatory.nasa.gov). The paleotsunami evidence also includes two predecessors to the Jogan event that also penetrated ~4 km inland (although in Jogan time, the shoreline was ~1 km west of present). These large tsunami support the existence of periodic outsized earthquakes ($M_w \sim 9$) along the Tohoku coast. The recurrence times are between 800 and 1200 years, with numerous smaller events between that make up the majority of the historical record (Shishikura *et al.*, 2007; Sawai *et al.*, 2008). Our field transect across the Ishinomaki Plain verifies the result of Shishikura and suggests that the Jogan tsunami deposits are locally more robust than even the March 2011 tsunami deposit, even accounting for coastline change, supporting the inference that Jogan may have been a $M_w \sim 9$ earthquake (Ⓔ Fig. S1, available as an electronic supplement to this paper).

In Hokkaido, a similar relationship has been observed between the shorter historical and instrumental records and the paleoseismic record along the northern Japan trench. Prehistoric tsunami that most likely were generated from long ruptures along the northern Japan trench were significantly larger than those generated by earthquakes of M_w 7–8.3 in the historical and instrumental records (Nanayama *et al.*, 2003). Over the past 2000–7000 years, such outsized events ($M_w \sim 9$) occurred on average about every 500 years in the Hokkaido region, with the most recent event ~350 years ago (Nanayama *et al.*, 2003).

HIMALAYAN FRONT AND HAIYUAN FAULT

The Himalayan front region experienced four earthquakes in the period 1897–1950 with magnitudes of 7.8–8.4 that have been assumed to be the maximum considered earthquake (MCE), or design earthquake, for power plants and large hydroelectric dams. However, surface rupture accompanying these four historic earthquakes was either absent or small (summarized by Yeats [2012]). On the other hand, paleoseismological evidence exists for surface displacements as large as 26 m from an earthquake in the late fifteenth to sixteenth century along the Himalayan front of northwest India (Kumar *et al.*, 2006) that may correspond to an earthquake in 1505 A.D. (Iyengar *et al.*, 1999). An earlier earthquake around 1100–1200 A.D. in Nepal and the adjacent Arunachal Pradesh state in northeast India (Fig. 2) was accompanied by a single-event surface rupture of 17 m or larger. Rupture lengths accompanying these earthquakes may be possibly the largest known worldwide on a continental reverse-fault earthquake (Lavé *et al.*, 2005; Kumar *et al.*, 2006, 2010; Fig. 2). Trenching of this fault supports a large single rupture, as opposed to several smaller events closely spaced in time. It has been suggested that the rupture length for both the 1505 A.D. and the 1100–1200 A.D. earthquakes might be close to 900 km (Kumar *et al.*, 2010; Yeats, 2012). A 900-km rupture length implies magnitudes greater than 8.5 (Wells and Coppersmith, 1994); however, uncertainty exists in the exact timing of these earthquakes due to uncertainty in correlating dates in trenches with historical events in both India and Nepal.

Another example of the contrast in inferred MCE based on recent historic information with longer-term geologic data is found along the Haiyuan fault in Gansu Province, China. This fault was the source of an earthquake in 1920 with a rupture length of 237 km that killed more than 220,000 people (Ⓔ Fig. S2 in the electronic supplement). An extensive paleoseismic trenching program along the entire length of the fault showed that the 1920 earthquake was not typical of this fault. Yongkang *et al.* (1997) divided the 1920 rupture into three segments and dated surface-rupturing earthquakes in each segment over the past 6000 years. They found that some earthquakes ruptured one segment, and some ruptured two, but only one prehistoric earthquake (6100–6200 years B.P.) ruptured all

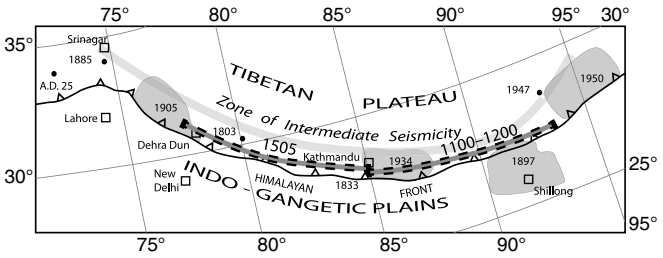

▲ **Figure 2.** Great earthquakes of the Himalayan front, showing meizoseismal zones of 1897, 1905, 1934, and 1950 earthquakes (ovals) and the extent of larger earthquakes in 1100–1200 and 1505 (heavy filled and dashed lines).

three segments and may have been a duplicate of the 1920 event (Yongkang *et al.*, 1997). In this example, the most recent earthquake was the largest, and prior to trenching, there was a tendency to regard the 1920 earthquake as the typical or characteristic earthquake. The paleoseismic evidence showed that the majority of the earthquakes were much smaller. Ⓔ Table S2 also shows that the two largest events had much greater net slip (5.6 and 7.0 m, respectively, for the ~6150 B.P. and A.D. 1920 events) than the 1.5–2 m average for the seven intervening single-segment ruptures (six additional single and one three-segment rupture could not be determined; Institute of Geology State Seismological Bureau and Seismological Bureau of Ningxia Hui Autonomous Region, 1990).

CASCADIA

In Cascadia, several decades of paleoseismic work have yielded an unprecedented record of great earthquakes. A pioneering work (Atwater, 1987) established the repeated occurrence of great earthquakes and tsunami along the Washington coast, followed by widespread evidence of subsidence and tsunami from coastal sediments along the entire margin from Canada to northern California (Clague and Bobrowsky, 1994; Atwater and Hemphill-Haley, 1997; Atwater *et al.*, 2003; Kelsey *et al.*, 2005). The longest records available, those from deep-sea turbidites, reveal the complex behavior of this subduction zone over the past 10,000 years (Goldfinger *et al.*, 2012; Ⓔ Fig. S3 in the electronic supplement). The offshore records are in good agreement with onshore paleoseismology during intervals, in which temporal overlap exists (less than ~4600 years B.P.), and both offer consistent information about the relative size of paleoearthquakes, giving confidence that both are recording the same phenomenon (Goldfinger *et al.*, 2012). The longer records reveal several important features not discernible with shorter records. One is that there is apparent clustering of the larger (rupture lengths greater than 600 km, M_w ~ 8.7–9.0) events into groups of four to five events, with 700- to 1200-year gaps between the clusters (Goldfinger *et al.*, 2012). Another is significant segmentation of the margin, with a group of shorter ruptures limited to southern Cascadia that are interspersed between the long ruptures as determined by intersite stratigraphic correlation (Goldfinger *et al.*, 2008, 2012, their fig. 55).

Evidence of the relative size of these great events comes from comparisons of turbidite thickness and rupture length using the extensive spatial sampling of the cores (Ⓔ Fig. S3 in the electronic supplement) and suggests that there may be earthquakes larger than the well-known A.D. 1700 M_w 9 event. Goldfinger *et al.* (2012) showed that mass per event down core among four key Cascadia core sites is reasonably consistent among sites. They inferred that the best explanation is that turbidite thickness and mass are linked to the relative levels of ground shaking in the source earthquakes. The magnitude of the A.D. 1700 earthquake is estimated to be ~9.0 based on tsunami inversion of the tsunami heights along the Japanese coast and the attribution of this "orphan tsunami" to Cascadia (Satake *et al.*, 2003). The 9.0 magnitude could change in the future with more sophisticated modeling, but it still provides a benchmark for other paleoseismic events. The connection between earthquake size and turbidite size is tenuous; nevertheless, the correlation between size characteristics per event, among numerous cores along strike, strongly suggests a regional connection that can best be attributed to the magnitude or shaking intensity of the source earthquake (Fig. 3; Goldfinger *et al.*, 2008, 2012). In the offshore turbidite record, the turbidite associated with the 1700 A.D. event is roughly "average" in mass and thickness relative to the 19 inferred similar ruptures as compared between core sites along the 1000-km Cascadia margin (Goldfinger *et al.*, 2012). Significantly, there are several turbidites that are considerably larger in terms of thickness and mass in the 10,000-year offshore record. Notable are the 11th and 16th events back in time, known as T11 and T16, that took place 5960 ± 140 and 8810 ± 160 years ago (Fig. 3). These two turbidites are consistently larger at all core sites along the length of Cascadia (Ⓔ Fig. S4 and Table S3 in the electronic supplement), being an average of 2.9 times (range 2.8–3.1) the A.D. 1700 turbidite mass. At most sites, four to seven other events in the 10 ky turbidite record (typically including turbidites T5, T6, T7, T8, T9, T13, and T18) are also larger than those in the 1700 A.D. turbidite, although by smaller margins of 1.3–1.7 times the T1 turbidite mass (range 0.2–1.7). Goldfinger *et al.* (2012) estimated M_w for all 19 Cascadia ruptures of 600 km and greater using estimated rupture length, width, and slip parameters calibrated to the A.D. 1700 event and setting that event equal to 9.0. They estimated M_w for T11 and T16 to be ~9.1. The average mass increase in these two turbidites of 2.8 times the A.D. 1700 turbidite is roughly comparable with the energy increase of 1.4 times from M_w 9.0 to M_w 9.1. The event-to-event variability and consistency among sites are unlikely to be due to changes in sediment supply, oceanography, or other factors as they are replicated at numerous sites, including one (Hydrate Ridge) with no modern terrigenous sediment supply. The outsized turbidites are unlikely to be due to a long prior sediment accumulation interval, as only T11 has such a prior interval (~1100 years interrupted by one small event), and because other events following ~1000-year gaps were not outsized in thickness or mass (T6 for example). These data suggest that significantly outsized earthquakes may occur at a rate of 1–2/10,000 years in Cascadia.

DISCUSSION

Uniquely, the 10-ky Holocene Cascadia-earthquake-generated turbidite stratigraphy affords uncommon opportunities to examine recurrence models, clustering, and detailed long-term (10 ky) strain history of a subduction zone. First, in Cascadia, the two outsized superquakes do not appear to occur in an otherwise random sequence. Cascadia earthquakes appear to cluster, with the larger events that include much of the strike length of the margin occurring within groupings of four to five events that comprise the four Holocene clusters. There appears to be a weak tendency to terminate these clusters with an

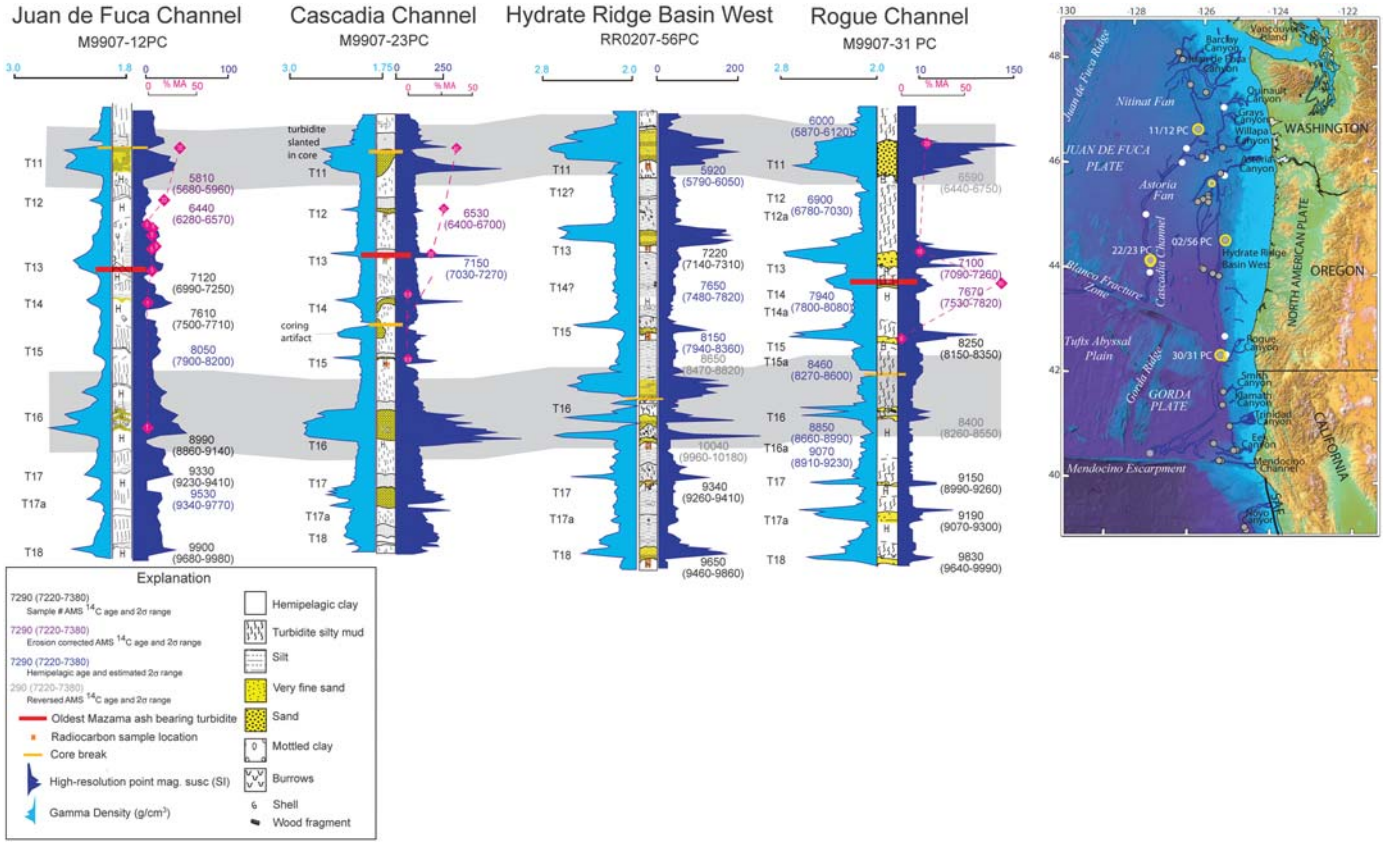

▲ **Figure 3.** Correlation of four Cascadia turbidite cores spanning 550 km of the Cascadia margin from regionally correlated turbidites in the work of Goldfinger *et al.* (2012). Events T11–T18 are shown to illustrate the two extreme events in this record, T11 and T16. T16 is a complex event with three elements at all sites, suggestive of shaking from three rupture patches in close succession. The three units in T16 are more widely spaced in proximal cores such as 56 PC. T16 also diminishes southward at Rogue Canyon. Location map shows the four cores in large yellow-bordered symbols. Red diamonds indicate Mazama Ash percent.

outsized event. The long time series also suggests that Cascadia is neither time nor slip predictable (Goldfinger *et al.*, 2012).

Because there appears to be a connection between earthquake size and turbidite size among core sites and across a variety of depositional environments, an opportunity exists to investigate the earthquake pattern further. This inference comes from the observation that correlated turbidites along strike in Cascadia vary considerably in mass and thickness per event at each site in the Holocene series but that they are consistent in mass and thickness for the same event at multiple sites and multiple depositional environments, as previously described (Goldfinger *et al.*, 2012; Ⓔ Fig. S4, Tables S4 and S5 in the electronic supplement). Because of this consistency for individual events along the margin, and despite the obvious simplifications involved, we infer that turbidite mass can be considered a crude proxy for seismic moment or intensity of ground shaking at offshore sites for at least the 19 larger ruptures of 600 km or greater described by Goldfinger *et al.* (2012).

If our assumption that energy release can be approximated by turbidite mass and thickness, we can then assemble and compare the Holocene series of earthquakes as a time series. First, we assume that although the slip and moment of paleoearthquakes are unknown, that coseismic energy release may be modeled as proportional to the mass of turbidites triggered in seismic shaking. Second, we assume that plate convergence between earthquakes increases elastic strain energy in proportion to interevent time (a coupling coefficient of 1.0 is assumed but does not affect the outcome).

To examine the energy balance between subduction earthquakes and accumulation of elastic strain, we scale turbidite mass (energy release) to balance plate convergence (energy gain) to generate a 10-ky energy time series for Cascadia (Fig. 4). We do not know the starting or ending values, of course; thus, we simply scale the plot such that the overall trend of the series has no net gain or loss of potential energy. The interval between the last earthquake and the next one is also unknown, and we set this equal to the average recurrence time. Sources of error also include the uncertainties in the radiocarbon ages for each event, which are taken from Goldfinger *et al.* (2012) and are shown on the plot. Both approximations undoubtedly comprise additional sources of error. The resulting sawtooth pattern reveals what we interpret as a complex pattern of long-term energy cycling on the Cascadia megathrust, with the vertical scale

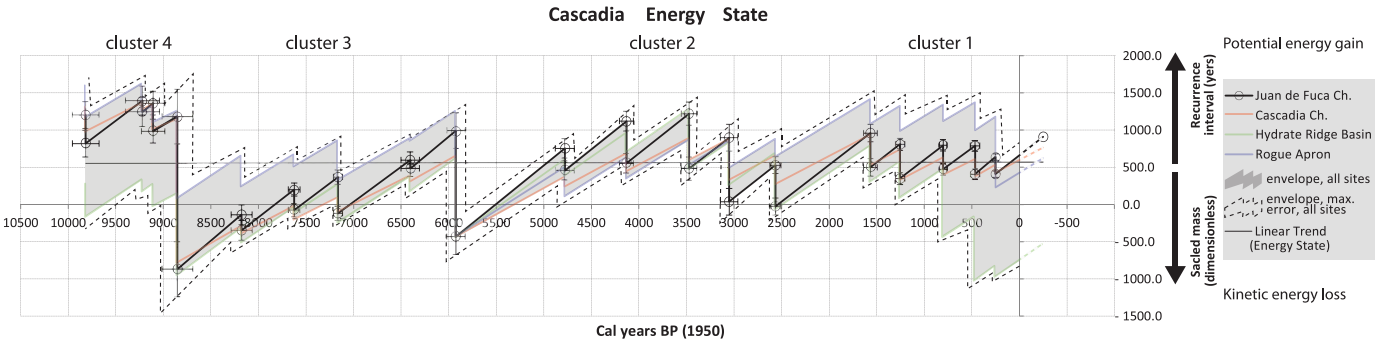

▲ **Figure 4.** Plot showing long-term energy cycling of the Cascadia megathrust, and complex behavior over time. The Cascadia Holocene earthquake time series at four primary sites is expressed as energy gain and loss per event. Energy gain is proportional to recurrence between events in years. Energy loss is proportional to the mass of turbidite samples, scaled to result in no net gain or loss of energy through the Holocene. Four primary sites are shown with envelope showing variability, and dashed line showing maximum variability including error. The four sites are pinned at large and consistent event T11 (~5900 cal BP) for comparison. Mass values are extracted from the gamma density curves, using as a baseline the mass values for each baseline pair of bounding hemipelagic layers. Mass values (dimensionless) are then DC scaled to yield net change when plotted against recurrence interval in years (see Ⓔ Fig. S6 in the electronic supplement for scale factors). Core compaction is partially compensated for by this method, though some unknown compaction error remains in this plot. Error ranges are OxCal (Bronk Ramsey, 2001) 2σ ranges from Goldfinger *et al.* (2012) in the X axis (time), and an estimated maximum value of 10% error applied to the mass values that includes possible air gaps in the core liner, bioturbation if present within the turbidites (rare), measurement error, error in establishing the baseline for each turbidite, and digitizing error. Final event assumed to occur 500 years from last event at AD 1700, a value equal to the average recurrence time (Goldfinger *et al.*, 2012). See Figure 3 and Ⓔ Fig. S3 in the electronic supplement for core locations. See Ⓔ Table 4 in the electronic supplement for radiocarbon data.

representing potential energy. If correct, we can then make some observations about the long-term behavior of Cascadia. Earthquake clusters including small to large events appear to have significant variations in energy balance within and between the clusters. Cluster 4 (~10,000–8800 B.P.) appears to maintain a relatively even energy state composed of several seismic cycles before falling to a low after large-event T16. Cluster 3 (~8200–5800 B.P.) climbs steadily in energy state through multiple seismic cycles until falling sharply to a similar low following large-event T11. Cluster 2 (~4800–2500 B.P.) climbs then falls to a low energy value after T6, which also precedes a long gap of ~1000 years, which then raises the energy state. Cluster 1 (~1600–300 B.P.) slowly declines from T5 to T1, the A.D. 1700 $M_w \sim 9.0$ earthquake.

Overall, what is suggested by this pattern is that some events release less energy, whereas others release more energy than available from plate convergence (slip deficit) and may have borrowed stored energy from previous cycles. This suggests that energy release in the earthquakes is not closely tied to recurrence intervals, that is, they are not obviously slip or time predictable, but the pattern of values suggests that it is not likely to be a Poisson process either. The highest energy states may result in either a very large earthquake or a series of smaller earthquakes to relieve stress. A very low energy state may result in a long gap or in a series of smaller earthquakes with a net energy gain over time, something that also appears to describe northeast Japan prior to the 2011 Tohoku earthquake. Although the starting and ending points in Figure 4 are unknown, and the scale factor is based only on the condition of no net energy change over 10,000 years, we note that changes in these three parameters cannot alter the pattern observed or make the series either time or slip predictable (Ⓔ Figs. S5 and S6 in the electronic supplement). Neither would a different value for the coupling coefficient alter the pattern. If we sum the seismic moment for Cascadia using the geographic dimensions and rates in the work of Goldfinger *et al.* (2012), the total seismic moment available is 6.7×10^{30} dyn · cm. If we then sum the inferred seismic moment from the individual events and their dimensions from the same source, the total is 6.1×10^{30} dyn · cm, implying a seismic coupling coefficient of ~0.9, although this is approximate at best. The seismic coupling coefficient, however, does not influence the result shown in Figure 3, unless this value varies from event to event, a possibility that cannot be ruled out. It is also possible that the 10,000 year time series is not long enough to estimate this parameter. We include a similar figure showing the hypothetical energy state in northeast Japan, based on paleoseismology and historical earthquakes in the rupture zone of the 2011 earthquake (Ⓔ Fig. S7 in the electronic supplement).

Long-term supercycles (Sieh *et al.*, 2008) may help explain observed mismatches between deformation-model-based paleoseismology and those based on geodetic and other datasets. For example, Bradley Lake, Oregon, is a tsunami deposit site in a coastal lake that provides an excellent sensitivity test of the energy generated by past earthquakes. Although the tsunami deposits in Bradley Lake are good temporal correlatives for offshore turbidites (Goldfinger *et al.*, 2012), the fault slip required to generate tsunami that reach the lake appears inconsistent with the time intervals between events. Tsunami models generated using the slip expected from plate motion for late

Holocene earthquake ruptures in the most recent cluster are 170–340 years. Yet, tsunami generated from full coupling of the North American and Juan de Fuca plates does not produce a large enough tsunami to reach the lake with these values (Witter *et al.*, 2012). Moving all parameters in the direction of a larger tsunami (broader locked interface, full rupture in deep water at the trench, and including a splay fault (which Witter *et al.* [2012] did not believe was significant) still failed to generate sufficient inundation (Witter *et al.*, 2012). This discrepancy may be explained by invoking a long-term cycle in which a series of earthquakes use long-term energy stored from previous seismic cycles (Goldfinger *et al.*, 2010; Witter *et al.*, 2012), or alternatively that some of the smaller events represent unbroken patches from previous heterogeneous ruptures (Witter *et al.*, 2012).

CONCLUSIONS

Collectively, data on the timing and size of geologically recorded earthquakes are not always consistent with the historic or instrumental record. It is becoming increasingly clear that our short instrumental and historical records are inadequate to characterize the complex and multiscale seismic behavior of subduction zones and other major fault systems. The recurrence intervals for superquakes and supercycles may be very long, potentially biasing the record from the start. The data presented here suggest that the types and sizes of large earthquakes a given fault system is capable of producing may be unknown for most major fault systems. This too is a function of the short histories available. This bias toward what we have observed or recorded directly has shaped the development of conceptual models such as the characteristic earthquake model, the seismic gap theory, the relationship between plate age and convergence velocity, and time and slip predictability.

Given recent failures of conceptual models of great earthquake recurrence, we must consider that there may not be reliable predictive factors available for such purposes at present or in the immediate future because many major fault systems lack both paleoseismology and GPS coverage. Evidence for deep coupling in northeast Japan (Kato, 1983; Ikeda, 2012; Ikeda *et al.*, 2012) and perhaps Cascadia (Chapman and Melbourne, 2009) suggests that our knowledge of plate coupling is also far from complete. Paleoseismology offers a relatively simple method of determining the long-term behavior of a fault system, in the best of circumstances providing information on not just the time series of event occurrences and current strain accumulation but also on segmentation, clustering, magnitudes, and stress transfer. The evidence here for strain supercycles that transcend individual seismic cycling is troubling even for short-term paleoseismic records. The paleoseismic data, however, can be helpful in eliminating seismic cycle scenarios that have never occurred while emphasizing those that did.

In terms of seismic hazards, particularly for critical facilities, we suggest that characterization of the MCE may require earthquake records over tens of past events, perhaps as long as 10,000 years. Credible earthquake scenarios that rely on instrumental or even relatively long historical records as in northeast Japan may or may not capture the range of earthquakes possible for a given fault system. Bias can occur in either direction, as the case of the 1920 $M_w \sim 7.8$ Haiyuan, China, earthquake, which was larger than most of the earthquakes on that fault, whereas the 2011 Tohoku event seemed outsized relative to recent history. Long records put both types of bias in perspective.

Superquakes appear to result from linkups of fault segments that more commonly have separate histories. These segments may connect in long ruptures in ways and at times that cannot presently be predicted. They may also result in larger slips and possibly broader ruptures, entraining regions of the fault less commonly utilized in smaller ruptures as likely happened in Tohoku, in the Haiyuan fault, and possibly in Cascadia. We suspect that elastic strain may accumulate at even very small rates in settings previously considered unfavorable, like a slow-charging battery, and that any such fault may be capable of eventually generating a very large earthquake using strain accumulated over many normal seismic cycles and may then still have considerable energy remaining for more earthquakes. Such long-term cycling is suggested for the Himalayan front, the Haiyuan fault, northeast Japan, and Cascadia, one of a very few localities where enough events are recognized to test such models over many supercycles. A similar relationship has been observed in Chile in the 1960 rupture zone (Cisternas *et al.*, 2005), Sumatra (Sieh *et al.*, 2008), and supercycles may explain the periodic occurrence of the observed outsized events in Hokkaido.

At a minimum, the Tohoku earthquake implies that comparable subduction zones, and perhaps others (McCaffrey, 2008), may be capable of similar behavior. A significant number of subduction zones have relatively old oceanic plates being subducted that were previously discounted as M 9 producers. These include much of South America north of the 1960 event (possibly represented by the 1868 Arica Chile earthquake; Dorbath *et al.*, 1990), the remainder of the Japan trench, the Kuriles, the western Aleutians, the Philippine, Manila and Sulu trenches, Java, the Makran and Hikurangi, Antilles, and others. Any or all of these subduction systems may be capable of generating earthquakes much larger than known or expected today.

ACKNOWLEDGMENTS

We thank Mary Lou Zoback for her thoughtful and detailed review that greatly improved the manuscript. The primary funding for field work and subsequent research has been provided by the National Science Foundation (NSF) Awards EAR 9803081, EAR-0001074, EAR-0107120, EAR-0440427, and OCE-0550843 (reservoir model development) and OCE 0850931 (2009 cruise). The U.S. Geological Survey substantially supported the work through Cooperative Agreements 6-7440-4790, 98HQAG2206, and 99HQAG0192 and the U.S. Geological Survey National Earthquake Hazard Reduction Program Grants 02HQGR0019, 03HQGR0037, 06HQGR0149,

and 07HQGR0064 to Goldfinger and 02HQGR0043, 03HQGR0006, and 06HQGR0020 to C. H. Nelson. The American Chemical Society awarded support to Ph.D. student Joel Johnson for core collection and analysis at Hydrate Ridge under ACS PRF 37688-AC8. Himalayan work was supported by NSF Grant EAR 0635987 to A. Meigs, D. Yule, and R.S. Yeats.

REFERENCES

Atwater, B. F. (1987). Evidence for great Holocene earthquakes along the outer coast of Washington State, *Science* **236,** 942–944.

Atwater, B. F., and E. Hemphill-Haley (1997). Recurrence intervals for great earthquakes of the past 3500 years at northeastern Willapa Bay, Washington, *U.S. Geological Survey*, Reston, Virginia, 108 pp.

Atwater, B. F., M. P. Tuttle, E. S. Schweig, C. M. Rubin, D. K. Yamaguchi, and E. Hemphill-Haley (2003). Earthquake recurrence inferred from paleoseismology, in *The Quaternary period in the United States*, A. R. Gillespie, S. C. Porter, and B. F. Atwater (Editors), Vol. 1, Elsevier, 331–350.

Bronk Ramsey, C. (2001). Development of the radiocarbon program OxCal, *Radiocarbon* **43,** 355–363.

Chapman, J. S., and T. I. Melbourne (2009). Future Cascadia megathrust rupture delineated by episodic tremor and slip, *Geophys. Res. Lett.* **36,** L22301, doi: 10.1029/2009GL040465.

Cisternas, M., B. F. Atwater, F. Torrejon, Y. Sawai, G. Machuca, M. Lagos, A. Eipert, C. Youlton, I. Salgado, T. Kamataki, M. Shishikura, C. P. Rajendran, J. Malik, and M. Husni (2005). Predecessors of the giant 1960 Chile earthquake, *Nature* **437,** 404–407.

Clague, J. J., and P. T. Bobrowsky (1994). Tsunami deposits beneath tidal marshes on Vancouver Island, British Columbia; with Suppl. Data 9421, *Geol. Soc. Am. Bull.* **106,** 1293–1303.

DeMets, C., R. G. Gordon, and D. F. Argus (2010). Geologically recent plate motions, *Geophys. J. Int.* **181,** 1–80.

Dorbath, L., A. Cisternas, and C. Dorbath (1990). Assessment of the size of large and great historical earthquakes in Peru, *Bull. Seismol. Soc. Am.* **80,** no. 3551–576.

Fujiwara, T., S. Kodaira, T. No, Y. Kaiho, N. Takahashi, and Y. Kaneda (2011). The 2011 Tohoku-oki earthquake: Displacement reaching the trench axis, *Science* **334,** 1240.

Geographical Information Authority of Japan (2010). Crustal Deformations of Entire Japan, *Report of Coordinating Committee for Earthquake Prediction, Japan*, Vol. 84, Geographical Information Authority of Japan, Tsukuba, Japan, 8–31 (in Japanese).

Goldfinger, C., K. Grijalva, R. Burgmann, A. E. Morey, J. E. Johnson, C. H. Nelson, J. Gutierrez-Pastor, A. Ericsson, E. Karabanov, J. D. Chaytor, J. Patton, and E. Gracia (2008). Late Holocene rupture of the northern San Andreas fault and possible stress linkage to the Cascadia subduction zone, *Bull. Seismol. Soc. Am.* **98,** 861–889.

Goldfinger, C., R. Witter, G. R. Priest, K. Wang, and Y. Zhang (2010). Cascadia supercycles: Energy management of the long Cascadia earthquake series, Presented at the *Annual Meeting of the SSA*, Portland, Oregon, April, 2010.

Goldfinger, C., C. H. Nelson, A. Morey, J. E. Johnson, J. Gutierrez-Pastor, A. T. Eriksson, E. Karabanov, J. Patton, E. Gracia, R. Enkin, A. Dallimore, G. Dunhill, and T. Vallier (2012). Turbidite event history: Methods and implications for Holocene Paleoseismicity of the Cascadia Subduction Zone, *U.S. Geol. Surv. Profess. Pap. 1661-F,* 184 pp.

Hashimoto, M. (1990). Horizontal strain rates in the Japanese Islands during interseismic period deduced from geodetic surveys (part I): Honshu, Shikoku and Kyushu, *Zisin* **43,** 13–26 (in Japanese with English abstract).

Igarashi, T. (2010). Spatial changes of inter-plate coupling inferred from sequences of small repeating earthquakes in Japan, *Geophys. Res. Lett.* **37,** L20304, doi: 10.1029/2010GL044609.

Ikeda, Y. (2003). Discrepancy between geologic and geodetic strain rates, *Chikyu (Earth Monthly)* **25,** no. 2, 125–129 (in Japanese).

Ikeda, Y. (2005). Long-term and short-term rates of horizontal shortening over the northeast Japan arc, Presented at the *Hokudan International Symposium on Active Faulting*, Hokudan City, Japan, January 2005.

Ikeda, Y. (2012). Long-term strain buildup in the northeast Japan arc–trench system and its implications for the gigantic subduction earthquake of March 11, 2011, in *Proc. of the International Symposium on Engineering Lessons Learned from the 2011 Great East Japan Earthquake*, Tokyo, Japan, 1–4 March 2012, 238–253, http://nisee.berkeley.edu/elibrary/Text/201204246.

Ikeda, Y., S. Okada, and M. Tajikara (2012). Long-term strain buildup in the northeast Japan arc–trench system and its implications for gigantic strain-release events, *J. Geol. Soc. Jpn.* **118,** 294–312 (in Japanese).

Institute of Geology State Seismological Bureau and Seismological Bureau of Ningxia Hui Autonomous Region (1990). *The Haiyuan Active Fault Zone*, Seismological Press, Beijing, 177–255 (in Chinese).

Iyengar, R. N., D. Sharma, and J. M. Siddiqui (1999). Earthquake history of India in medieval times, *Indian J. Hist. Sci.* **34,** no. 3, 181–237.

Kato, T. (1983). Secular and earthquake-related vertical crustal movements in Japan as deduced from tidal records (1951–1981), *Tectonophysics* **97,** 183–200.

Kelsey, H. M., A. R. Nelson, E. Hemphill-Haley, and R. C. Witter (2005). Tsunami history of an Oregon coastal lake reveals a 4600 yr record of great earthquakes on the Cascadia subduction zone, *Geol. Soc. Am. Bull.* **117,** nos. 7–8, 1009–1032.

Koike, K., and H. Machida (2001). *Atlas of Marine Terraces of Japan*, University of Tokyo Press, Japan, 105 pp.

Kumar, S., S. G. Wesnousky, R. Jayangondaperumal, T. Nakata, Y. Kumahara, and V. Singh (2010). Paleoseismological evidence of surface faulting along the northeastern Himalayan front, India: Timing, size, and spatial extent of great earthquakes, *J. Geophys. Res.* **115,** B12422.

Kumar, S., S. G. Wesnousky, T. K. Rockwell, R. W. Briggs, V. C. Thakur, and R. Jayangondaperumal (2006). Paleoseismic evidence of great surface rupture earthquakes along the Indian Himalaya, *J. Geophys. Res.* **111,** B03304, doi: 10.1029/2004JB003309.

Lavé, J., D. Yule, S. Sapkota, K. Basant, C. Madden, M. Attal, and R. Pandey (2005). Evidence for a great medieval earthquake (~1100 A.D.) in the Central Himalayas, Nepal, *Science* **307,** 1302–1305.

McCaffrey, R. (2007). The next great earthquake, *Science* **315,** 1675–1676.

McCaffrey, R. (2008). Global frequency of magnitude 9 earthquakes, *Geology* **36,** 263–266.

Minoura, K., F. Imamura, D. Sugawara, Y. Kono, and T. Iwashita (2001). The 869 Jogan tsunami deposit and recurrence interval of large-scale tsunami on the Pacific coast of northeast Japan, *J. Nat. Disast. Sci.* **23,** no. 2, 83–88.

Namegaya, Y., K. Satake, and S. Yamamoto (2010). Numerical simulation of the A.D. 869 Jogan tsunami in Ishinomaki and Sendai plains and Ukedo river-mouth lowland. Annual report on active faults and paleoearthquake researches, *Geol. Surv. Jpn.* **10,** 9–29 (in Japanese with English abstract).

Nanayama, F., K. Satake, R. Furukawa, K. Shimokawa, B. F. Atwater, K. Shigeno, and S. Yamaki (2003). Unusually large earthquakes inferred from tsunami deposits along the Kuril trench, *Nature* **424,** 660–663.

Okada, S., and Y. Ikeda (2012). Quantifying crustal extension and shortening in the back-arc region of northeast Japan, *J. Geophys. Res.* **117,** B01404, 28 pp., doi: 10.1029/2011JB008355.

Ruff, L. J. (1989). Do trench sediments affect great earthquake occurrence in subduction zones? *Pure Appl. Geophys.* **129,** 263–282.

Ruff, L., and H. Kanamori (1980). Seismicity and the subduction process, *Phys. Earth Planet. In.* **23,** 240–252.

Sagiya, T., S. Miyazaki, and T. Tada (2000). Continuous GPS array and present-day crustal deformation of Japan, *Pure Appl. Geophys.* **157,** 2303–2322.
Satake, K., K. Wang, and B. F. Atwater (2003). Fault slip and seismic moment of the 1700 Cascadia earthquake inferred from Japanese tsunami descriptions, *J. Geophys. Res.* **108,** 2325.
Sato, H. (1989). Degree of deformation of late Cenozoic strata in the Northeast Honshu Arc, *Memoir Geol. Soc. Jpn.* **32,** 257–268 (in Japanese with English abstract).
Sato, H. (1994). The relationship between Late Cenozoic tectonic events and stress-field and basin development in northeast Japan, *J. Geophys. Res.* **99,** 22,261–22,274.
Sato, M., T. Ishikawa, N. Ujihara, S. Yoshida, M. Fujita, M. Mochizuke, and A. Asada (2011). Displacement above the hypocenter of the 2011 Tohoku–Oki Earthquake, Science **332,** 1395.
Sawai, Y., M. Shishikura, Y. Okamura, K. Takada, T. Matsu'ura, T. Aung, J. Komatsubara, Y. Fujii, O. Fujiwara, K. Satake, T. Kamataki, and N. Sato (2007). A Study on Paleotsunami Using Handy Geoslicer in Sendai Plain (Sendai, Natori, Iwanuma, Watari, and Yamamoto), Miyagi, Japan, *Tech. Report No. 7*, Geological Survey of Japan, AIST, National Institute of Advanced Industrial Science and Technology, Tsukuba, Japan, 31–46.
Sawai, Y., M. Shishikura, and J. Komatsubara (2008). A study on paleotsunami using hand corer in Sendai Plain (Sendai City, Natori City, Iwanuma City, Watari Town, Yamamoto Town), Miyagi, Japan. Annual report on active faults and paleoearthquake researches, *Geol. Surv. Jpn.* **8,** 17–70 (in Japanese with English abstract).
Scholz, C., and J. Campos (1995). On the mechanism of seismic decoupling and back arc spreading at subduction zones, *J. Geophys. Res.* **100,** 22,103–122,115.
Shishikura, M., Y. Sawai, Y. Okamura, J. Komatsubara, T. Tin Aung, T. Ishiyama, O. Fujiwara, and S. Fujino (2007). Age and distribution of tsunami deposit in the Ishinomaki Plain, northeast Japan, *Annual Rept. Active Fault Paleoearthq. Res.*, **7,** 31–46 (in Japanese with English abstract).
Sieh, K., D. H. Natawidjaja, A. J. Meltzner, C.-C. Shen, H. Cheng, K.-S. Li, B. W. Suwargadi, J. Galetzka, B. Philibosian, and R. L. Edwards (2008). Earthquake supercycles inferred from sea-level changes recorded in the corals of West Sumatra, *Science* **322,** no. 5908, 1674–1678.
Sugawara, D., K. Goto, F. Imamura, H. Matsumoto, and K. Minoura (2012). Assessing the magnitude of the 869 Jogan tsunami using sedimentary deposits: Prediction and consequence of the 2011 Tohoku–Oki tsunami, *Sediment. Geol.* **282,** 14–26.
Suwa, Y., S. Miura, A. Hasegawa, T. Sato, and K. Tachibana (2006). Interplate coupling beneath NE Japan inferred from three-dimensional displacement field, *J. Geophys. Res.* **111,** B04402, 12, doi: 10.1029/2004JB003203.
Tajikara, M. (2004). Vertical crustal movements of the northeast Japan arc in Late Quaternary time, *Ph.D. Thesis*, University of Tokyo, 159 pp.
Tajikara, M., and Y. Ikeda (2005). Vertical crustal movements and development of basin and range topography in the middle part of the northeast Japan arc estimated by fluvial/marine terrace data, *Quaternary Res.* **44,** 229–245 (in Japanese with English abstract).
von Huene, R., and S. Lallemand (1990). Tectonic erosion along the Japan and Peru convergent margins, *Geol. Soc. Am. Bull.* **102,** no. 6, 704–720, doi: 10.1130/0016-7606(1990)102<0704:teatja>2.3.co;2.
Wells, D. L., and K. J. Coppersmith (1994). New empirical relationships among magnitude, rupture length, rupture width, rupture area, and surface displacement, *Bull. Seismol. Soc. Am.* **84,** 974–1002.
Wesnousky, S. G., C. H. Scholtz, and K. Shimazaki (1982). Deformation of an island arc: rates of moment release and crustal shortening in intraplate Japan determined from seismicity and Quaternary fault data, *J. Geophys. Res.* **87,** 6829–6852.
Witter, R. C., Y. Zhang, K. Wang, C. Goldfinger, G. R. Priest, and J. C. Allan (2012). Coseismic slip on the southern Cascadia megathrust implied by tsunami deposits in an Oregon lake and earthquake-triggered marine turbidites, *J. Geophys. Res.* **117,** no. B10, B10303.
Yeats, R. S. (2012). *Active Faults of the World*, Cambridge University Press, Cambridge, U.K., 634 pp.
Yongkang, R., R. Duan, Q. Deng, D. Jiao, and W. Min (1997). 3D trench excavation and paleoseismology at Gaowanzi of the Haiyuan fault, *Seismol. Earthq.* **19,** no. 2, 97–107 (in Chinese).

Chris Goldfinger
Oregon State University
College of Earth, Ocean, and Atmospheric Sciences
104 Ocean Admin. Bldg.
Corvallis, Oregon 97331-5506 U.S.A.
gold@coas.oregonstate.edu

Yasutaka Ikeda
Department of Earth and Planetary Science
University of Tokyo
Hongo 7-3-1, Bunkyo-ku
Tokyo 113-0033, Japan
ikeda@eps.s.u-tokyo.ac.jp

Robert S. Yeats[1]
Department of Geosciences
Oregon State University
104 Wilkinson Hall
Corvallis, Oregon 97331-5506 U.S.A.
yeatsr@geo.oregonstate.edu

Junjie Ren
Key Laboratory of Crustal Dynamics
Institute of Crustal Dynamics
China Earthquake Administration
Beijing 100085, China
renjunjie@gmail.com

[1] Also at Earth Consultants International, 1642 East Fourth Street, Santa Ana, California 92701-5148 U.S.A.